

# A Model for Multiple scattering in Geant4

**László Urbán**

RMKI Research Institute for Particle and Nuclear Physics  
H-1525 Budapest, P.O. Box 49, Hungary  
laszlo.urban@cern.ch

December 11, 2006

## **Abstract**

We present a model to simulate the multiple scattering of charged particles in matter. The model is based on Lewis theory; it does not use the Moliere formalism. It simulates the scattering of a charged particle after a given step, computes the path length correction and the lateral displacement as well. This model is used in Geant4.

*Key Words:* Geant4 simulation multipleScattering

## **1 Introduction**

The MSC simulation algorithms can be classified into two different classes, *detailed* and *condensed* simulation. In the detailed simulation all the collisions/interactions experienced by the particle are simulated. This simulation can be considered as exact, i.e. it gives the same results as the solution of the transport equation, but it can be used only if the number of collisions is not too large. This condition fulfils only if the kinetic energy of the particle is low enough or for special geometry (thin foil). For larger kinetic energies the average number of collisions are very large and the detailed simulation becomes very inefficient. The high energy simulation codes use condensed simulation algorithms, where the global effects of the collisions is simulated after a track segment. The global effects generally computed in these codes are the net displacement, energy loss and change of direction of the charged particle. These quantities are computed from the multiple scattering theories used in the codes. The accuracy of these condensed simulations is limited



by the approximations of the multiple scattering theories.

Most of the particle physics simulation codes use the multiple scattering theories due to Molière ([2]), Goudsmit and Saunderson ([4]) and Lewis ([5]). The theories of Molière and Goudsmit-Saunderson give only the angular distribution after a step, while the Lewis theory computes the moments of the spatial distribution as well. None of these MSC theories gives the probability distribution of the spatial displacement therefore each of the MSC simulation codes incorporates its own algorithm to determine the spatial displacement of the charged particle after a given step. These algorithms are not exact and they give the main uncertainties of the MSC codes. Therefore the simulation results can depend on the value of the step length and generally one has to select the value of the step length carefully.

A new class of MSC simulation appeared in the literature recently, the *mixed* simulation algorithms (see e.g.[3]). The mixed algorithm simulates the *hard* collisions one by one and uses a MSC theory to treat the effects of the *soft* collisions after a given step. The number of the steps can be kept not very large in these algorithms and the dependence on the step length can be reduced, too.

The MSC model used in Geant4 belongs to the class of the condensed simulations. The model is based on the Lewis' MSC theory. It uses model functions to determine the angular and spatial distributions after a step. The functions have been chosen in such a way that they give the same moments of the (angular and spatial) distributions than the Lewis theory.

## 2 The model

### 2.1 Definition of Terms

In simulation, a particle is transported by steps through the detector geometry. The shortest distance between the endpoints of a step is called the *geometrical path length*,  $z$ . In the absence of a magnetic field, this is a straight line. For non-zero fields,  $z$  is the shortest distance along a curved trajectory. Constraints on  $z$  are imposed when particle tracks cross volume boundaries. The path length of an actual particle, however, is usually longer than the geometrical path length, due to physical interactions like multiple scattering. This distance is called the *true path length*,  $t$ . Constraints on  $t$  are imposed by the physical processes acting on the particle.

The properties of the multiple scattering process are completely determined by the *transport mean free paths*,  $\lambda_k$ , which are functions of the energy in a given material. The  $k$ -th transport mean free path is defined as

$$\frac{1}{\lambda_k} = 2\pi n_a \int_{-1}^1 [1 - P_k(\cos\chi)] \frac{d\sigma(\chi)}{d\Omega} d(\cos\chi) \quad (1)$$

where  $d\sigma(\chi)/d\Omega$  is the differential cross section of the scattering,  $P_k(\cos\chi)$  is the  $k$ -th Legendre polynomial, and  $n_a$  is the number of atoms per volume.

Most of the mean properties of MSC computed in the simulation codes depend only on the first and second transport mean free paths. The mean value of the geometrical path length (first moment) corresponding to a given true path length  $t$  is given by

$$\langle z \rangle = \lambda_1 \left[ 1 - \exp\left(-\frac{t}{\lambda_1}\right) \right] \quad (2)$$

Eq. 2 is an exact result for the mean value of  $z$  if the differential cross section has axial symmetry and the energy loss can be neglected. The transformation between true and geometrical path lengths is called the *path length correction*. This formula and other expressions for the first moments of the spatial distribution were taken from either [3] or [6], but were originally calculated by Goudsmit and Saunderson [4] and Lewis [5].

At the end of the true step length,  $t$ , the scattering angle is  $\theta$ . The mean value of  $\cos\theta$  is

$$\langle \cos\theta \rangle = \exp\left[-\frac{t}{\lambda_1}\right] \quad (3)$$

The variance of  $\cos\theta$  can be written as

$$\sigma^2 = \langle \cos^2\theta \rangle - \langle \cos\theta \rangle^2 = \frac{1 + 2e^{-2\kappa\tau}}{3} - e^{-2\tau} \quad (4)$$

where  $\tau = t/\lambda_1$  and  $\kappa = \lambda_1/\lambda_2$ .

The mean lateral displacement is given by a more complicated formula [3], but this quantity can also be calculated relatively easily and accurately. The square of the *mean lateral displacement* is

$$\langle x^2 + y^2 \rangle = \frac{4\lambda_1^2}{3} \left[ \tau - \frac{\kappa + 1}{\kappa} + \frac{\kappa}{\kappa - 1} e^{-\tau} - \frac{1}{\kappa(\kappa - 1)} e^{-\kappa\tau} \right] \quad (5)$$

Here it is assumed that the initial particle direction is parallel to the the  $z$  axis.

The lateral correlation is determined by the equation

$$\langle xv_x + yv_y \rangle = \frac{2\lambda_1}{3} \left[ 1 - \frac{\kappa}{\kappa - 1} e^{-\tau} + \frac{1}{\kappa - 1} e^{-\kappa\tau} \right] \quad (6)$$

where  $v_x$  and  $v_y$  are the x and y components of the direction unit vector. This equation gives the correlation strength between the final lateral position and final direction.

The transport mean free path values have been calculated by Liljequist et al. [7], [8] for electrons and positrons in the kinetic energy range 100 eV - 20 MeV in 15 materials. The MSC model in Geant4 uses these values for kinetic energies below 10 MeV. For high energy particles (above 10 MeV) the transport mean free path values have been taken from a paper of R.Mayol and F.Salvat ([9]). When necessary, the model linearly interpolates or extrapolates the transport cross section,  $\sigma_1 = 1/\lambda_1$ , in atomic number  $Z$  and in the square of the particle velocity,  $\beta^2$ . The ratio  $\kappa$  is a very slowly varying function of the energy:  $\kappa > 2$  for  $T >$  a few keV, and  $\kappa \rightarrow 3$  for very high energies (see [6]). Hence, a constant value of 2.5 is used in the model.

Nuclear size effects are negligible for low energy particles and they are accounted for in the Born approximation in [9], so there is no need for extra corrections of this kind in the model.

## 2.2 Path Length Correction

As mentioned above, the path length correction refers to the transformation true path length  $\rightarrow$  geometrical path length and its inverse. The true path length  $\rightarrow$  geometrical path length transformation is given by eq. 2 if the step is small and the energy loss can be neglected. If the step is not small the energy dependence makes the transformation more complicated. For this case Eqs. 3,2 should be modified as

$$\langle \cos\theta \rangle = \exp \left[ - \int_0^t \frac{du}{\lambda_1(u)} \right] \quad (7)$$

$$\langle z \rangle = \int_0^t \langle \cos\theta \rangle_u du \quad (8)$$

where  $\theta$  is the scattering angle,  $t$  and  $z$  are the true and geometrical path lengths, and  $\lambda_1$  is the transport mean free path.

In order to compute Eqs. 7,8 the  $t$  dependence of the transport mean free path must be known.  $\lambda_1$  depends on the kinetic energy of the particle which decreases along the step. All computations in the model use a linear approximation for this  $t$  dependence:

$$\lambda_1(t) = \lambda_{10}(1 - \alpha t) \quad (9)$$

Here  $\lambda_{10}$  denotes the value of  $\lambda_1$  at the start of the step, and  $\alpha$  is a constant. It is worth noting that Eq. 9 is *not* a crude approximation. It is rather good at low ( $< 1$  MeV) energy. At higher energies the step is generally much smaller than the range of the particle, so the change in energy is small and so is the change in  $\lambda_1$ . Using Eqs. 7 - 9 the explicit formula for the  $\langle \cos\theta \rangle$  and  $\langle z \rangle$  are :

$$\langle \cos\theta \rangle = (1 - \alpha t)^{\frac{1}{\alpha\lambda_{10}}} \quad (10)$$

$$\langle z \rangle = \frac{1}{\alpha(1 + \frac{1}{\alpha\lambda_{10}})} \left[ 1 - (1 - \alpha t)^{1 + \frac{1}{\alpha\lambda_{10}}} \right] \quad (11)$$

The value of the constant  $\alpha$  can be expressed using  $\lambda_{10}$  and  $\lambda_{11}$  where  $\lambda_{11}$  is the value of the transport mean free path at the end of the step

$$\alpha = \frac{\lambda_{10} - \lambda_{11}}{t\lambda_{10}} \quad (12)$$

At low energies (  $T_{kin} < M$ ,  $M$  is particle mass)  $\alpha$  has a simpler form:

$$\alpha = \frac{1}{r_0} \quad (13)$$

where  $r_0$  denotes the range of the particle at the start of the step.

It can easily be seen that for a small step (i.e. for a step with small relative energy loss) the formula of  $\langle z \rangle$  is

$$\langle z \rangle = \lambda_{10} \left[ 1 - \exp\left(-\frac{t}{\lambda_{10}}\right) \right] \quad (14)$$

Eq. 11 or 14 gives the mean value of the geometrical step length for a given true step length.

The actual geometrical path length can be sampled in the model according to the simple probability density function defined for  $v = z/t \in [0, 1]$  :

$$f(v) = (k+1)(k+2)v^k(1-v) \quad (15)$$

The value of the exponent  $k$  is computed from the requirement that  $f(v)$  must give the same mean value for  $z = vt$  as eq. 11 or 14. Hence

$$k = \frac{3\langle z \rangle - t}{t - \langle z \rangle} \quad (16)$$

The value of  $z = vt$  is sampled using  $f(v)$  if  $k > 0$ , otherwise  $z = \langle z \rangle$  is used.

The geometrical path length  $\rightarrow$  true path length transformation is performed using the mean values. The transformation can be written as

$$t(z) = \langle t \rangle = -\lambda_1 \log \left( 1 - \frac{z}{\lambda_1} \right) \quad (17)$$

is the geometrical step is small and

$$t(z) = \frac{1}{\alpha} \left[ 1 - (1 - \alpha w z)^{\frac{1}{w}} \right] \quad (18)$$

where

$$w = 1 + \frac{1}{\alpha \lambda_{10}}$$

if the step is not small, i.e. the energy loss should be taken into account.

This transformation is needed when the particle arrives at a volume boundary, causing the step to be geometry-limited. In this case the true path length should be computed in order to have the correct energy loss of the particle after the step.

## 2.3 Angular Distribution

The quantity  $u = \cos \theta$  is sampled according to a model function  $g(u)$ . The functional form of  $g$  is

$$g(u) = p[qg_1(u) + (1-q)g_2(u)] + (1-p)g_3(u) \quad (19)$$

where  $0 \leq p, q \leq 1$ , and the  $g_i$  are simple functions of  $u = \cos \theta$ , normalized over the range  $u \in [-1, 1]$ . The functions  $g_i$  have been chosen as

$$g_1(u) = C_1 e^{-a(1-u)} \quad -1 \leq u_0 \leq u \leq 1 \quad (20)$$

$$g_2(u) = C_2 \frac{1}{(b-u)^d} \quad -1 \leq u \leq u_0 \leq 1 \quad (21)$$

$$g_3(u) = C_3 \quad -1 \leq u \leq 1 \quad (22)$$

where  $a > 0$ ,  $b > 0$ ,  $d > 0$  and  $u_0$  are model parameters, and the  $C_i$  are normalization constants. It is worth noting that for small scattering angles  $g_1(u)$  is nearly Gaussian ( $\exp(-\theta^2/2\theta_0^2)$ ) if  $\theta_0^2 \approx 1/a$ , while  $g_2(u)$  has a Rutherford-like tail for large  $\theta$  if  $b \approx 1$  and  $d$  is not far from 2.

## 2.4 Determination of the Model Parameters

The parameters  $a$ ,  $b$ ,  $d$ ,  $u_0$  and  $p$ ,  $q$  are not independent. The requirement that the angular distribution function  $g(u)$  and its first derivative be continuous at  $u = u_0$  imposes two constraints on the parameters:

$$p g_1(u_0) = (1 - p) g_2(u_0) \quad (23)$$

$$p a g_1(u_0) = (1 - p) \frac{d}{b - u_0} g_2(u_0) \quad (24)$$

A third constraint comes from Eq. 7 :  $g(u)$  must give the same mean value for  $u$  as the theory.

It follows from Eqs. 10 and 19 that

$$q\{p\langle u \rangle_1 + (1 - p)\langle u \rangle_2\} = [1 - \alpha t]^{\frac{1}{\alpha\lambda_{10}}} \quad (25)$$

where  $\langle u \rangle_i$  denotes the mean value of  $u$  computed from the distribution  $g_i(u)$ .

The parameter  $a$  was chosen according to a modified Highland-Lynch-Dahl formula for the width of the angular distribution [10], [11].

$$a = \frac{0.5}{1 - \cos(\theta_0)} \quad (26)$$

where  $\theta_0$  is

$$\theta_0 = \frac{13.6 \text{ MeV}}{\beta c p} z_{ch} \sqrt{\frac{t}{X_0}} \left[ 1 + 0.038 \ln \left( \frac{t}{X_0} \right) \right] \quad (27)$$

when the original Highland-Lynch-Dahl formula is used. Here  $\theta_0 = \theta_{plane}^{rms}$  is the width of the approximate Gaussian projected angle distribution,  $p$ ,  $\beta c$  and  $z_{ch}$  are the momentum, velocity and charge number of the incident particle, and  $t/X_0$  is the true path length in radiation length unit. This value of

$\theta_0$  is from a fit to the Molière distribution for singly charged particles with  $\beta = 1$  for all  $Z$ , and is accurate to 11 % or better for  $10^{-3} \leq t/X_0 \leq 100$  (see e.g. Rev. of Particle Properties, section 23.3).

The modified formula for  $\theta_0$  is

$$\theta_0 = \frac{13.6 \text{ MeV}}{\beta_{cp}} z_{ch} \sqrt{\frac{t}{X_0}} \left[ 1 + 0.105 \ln \left( \frac{t}{X_0} \right) + 0.0035 \left( \ln \left( \frac{t}{X_0} \right) \right)^2 \right]^{\frac{1}{2}} f(Z) \quad (28)$$

where

$$f(Z) = 1 - \frac{0.24}{Z(Z+1)} \quad (29)$$

is an empirical correction factor based on high energy proton scattering data [17]. This formula gives a much smaller step dependence in the angular distribution and describes the available electron scattering data better than the Highland form.

The value of the parameter  $u_0$  has been chosen as

$$u_0 = 1 - \frac{\xi}{a} \quad (30)$$

where  $\xi$  is a constant ( $\xi = 3$ ).

The parameter  $d$  is set to

$$d = 2.40 - 0.027 Z^{\frac{2}{3}} \quad (31)$$

This (empirical) expression is obtained comparing the simulation results to the data of the MuScat experiment [18].

The remaining three parameters can be computed from Eqs. 23 - 25. The numerical value of the parameters can be found in the code.

It should be noted that in this model there is no step limitation originating from the multiple scattering process. Another important feature of this model is that the sum of the 'true' step lengths of the particle, that is, the total true path length, does not depend on the length of the steps. Most algorithms used in simulations do not have these properties.

In the case of heavy charged particles ( $\mu$ ,  $\pi$ ,  $p$ , etc.) the mean transport free path is calculated from the electron or positron  $\lambda_1$  values with a 'scaling'



applied. This is possible because the transport mean free path  $\lambda_1$  depends only on the variable  $P\beta c$ , where  $P$  is the momentum, and  $\beta c$  is the velocity of the particle.

In its present form the model samples the path length correction and angular distribution from model functions, while for the lateral displacement and the lateral correlation only the mean values are used and all the other correlations are neglected. However, the model is general enough to incorporate other random quantities and correlations in the future.

### 3 MSC simulation in Geant4

The step length of the particles is determined by the physics processes or the geometry of the detectors. The tracking/stepping algorithm checks all the step lengths demanded by the (continuous or discrete) physics processes and determines the minimum of these step lengths.

Then, this minimum step length must be compared with the length determined by the geometry of the detectors and one has to select the minimum of the 'physics step length' and the 'geometrical step length' as the actual step length.

This is the point where the MSC model comes into the game. All the physics processes use the true path length  $t$  to sample the interaction point, while the step limitation originated from the geometry is a geometrical path length  $z$ . The MSC algorithm transforms the 'physics step length' into a 'geometrical step length' before the comparison of the two lengths. This ' $t \rightarrow z$ ' transformation can be called as the inverse of the path length correction.

After the actual step length has been determined and the particle relocation has been performed the MSC performs the transformation ' $z \rightarrow t$ ', because the energy loss and scattering computation need the true step length ' $t$ '.

The scattering angle  $\theta$  of the particle after the step of length ' $t$ ' is sampled according to the model function given in eq. 19 . The azimuthal angle  $\phi$  is generated uniformly in the range  $[0, 2\pi]$ .

After the simulation of the scattering angle, the lateral displacement is computed using eq. 5. Then the correlation given by eq. 6 is used to determine the direction of the lateral displacement. Before 'moving' the particle accord-

ing to the displacement a check is performed to ensure that the relocation of the particle with the lateral displacement does not take the particle beyond the volume boundary.

### 3.1 Step Limitation Algorithm

In Geant4 the boundary crossing is treated by the transportation process ([1]). The transportation ensures that the particle does not penetrate in a new volume without stopping at the boundary, it restricts the step size when the particle leaves a volume. However, this step restriction can be rather weak in big volumes and this fact can result a not very good angular distribution after the volume. At the same time, there is no similar step limitation when a particle enters a volume and this fact does not allow a good backscattering simulation for low energy particles. Low energy particles penetrate too deeply into the volume in the first step and then - because of energy loss - they are not able to reach again the boundary in backward direction.

A very simple step limitation algorithm has been implemented in the MSC code to cure this situation. At the start of a track or after entering in a new volume, the algorithm restricts the step size to a value

$$f_r \cdot \max\{r, \lambda_1\} \quad (32)$$

where  $r$  is the range of the particle,  $f_r$  is a constant ( $f_r \in [0, 1]$ ); taking the max of  $r$  and  $\lambda_1$  is an empirical choice. In order not to use very small - unphysical - step sizes a lower limit is given for the step size as

$$tlimitmin = \max \left[ \frac{\lambda_1}{nstepmax}, \lambda_{elastic} \right] \quad (33)$$

where  $nstepmax = 25$  and  $\lambda_{elastic}$  is the mean free path of the elastic scattering (see later).

It can be easily seen that this kind of step limitation means a real constraint only for low energy particles.

In order not to allow for a particle to cross a volume in just one step, another limitation is implemented too. The limitation is the following: after entering a volume the step size can not be bigger than

$$\frac{d_{geom}}{f_g} \quad (34)$$

where  $d_{geom}$  is the distance to the next boundary (in the direction of the particle) and  $f_g$  is a constant parameter. The similar restriction at the start of a track is

$$\frac{2d_{geom}}{f_g} \quad (35)$$

The choice of the parameters  $f_r$  and  $f_g$  is a question related with performance too. By default  $f_r = 0.02$  and  $f_g = 2.5$  are used, but the parameters can be set to any other value in a simple way. One can get an approximate simulation of the backscattering with the default value, while if a better backscattering simulation is needed it is possible to get it using a smaller value for  $f_r$ . However, this model is very simple and it can reproduce the backscattering data approximately only.

### 3.2 Boundary Crossing Algorithm

A special stepping algorithm has been implemented recently (Autumn 2006) in order to improve the simulation around interfaces. This algorithm does not allow a 'big' last step(s) in a volume: the last step(s) can not be bigger than the mean free path of the elastic scattering of the particle in the given volume (material). After the last step(s) the particle scattered according to a single scattering law (i.e. there is no multiple scattering very close to the boundary or at the boundary).

The key parameter of the algorithm is the variable called *skin*. The algorithm is not active for  $skin \leq 0$ , while for  $skin > 0$  it is active in a layer of thickness  $skin \cdot \lambda_{elastic}$ . In this active layer the particle performs steps of length  $\lambda_{elastic}$  (or smaller if the volume boundary is closer than this value).

The scattering at the end of a small step is single or plural and for these small steps there are no path length correction and lateral displacement computation. In other words the program works in this thin layer in 'microscopic mode'.

The elastic mean free path can be estimated as

$$\lambda_{elastic} = \lambda_1 \cdot rat(T_{kin}) \quad (36)$$

where  $rat(T_{kin})$  a simple empirical function computed from the elastic and first transport cross section values of Mayol and Salvat [9]

$$rat(T_{kin}) = \frac{0.001(MeV)^2}{T_{kin}(T_{kin} + 10MeV)} \quad (37)$$

$T_{kin}$  is the kinetic energy of the particle.

At the end of a small step the number of scatterings is sampled according to the Poissonian distribution with a mean value  $t/\lambda_{elastic}$  and in the case of plural scattering the final scattering angle is computed by summing the contributions of the individual scatterings.

The single scattering is determined by the distribution

$$g(u) = C \frac{1}{(1 + 0.5a^2 - u)^2} \quad (38)$$

where  $u = \cos(\theta)$ ,  $a$  is the screening parameter,  $C$  is a normalization constant. The form of the screening parameter is

$$a = \frac{\alpha Z^{1/3}}{\sqrt{(\tau(\tau + 2))}} \quad (39)$$

where  $Z$  is the atomic number,  $\tau$  is the kinetic energy measured in particle mass units,  $\alpha$  is a constant. It can be shown easily that the function  $g(u)$  for small scattering angle  $\theta$  is equivalent with the well known formula of the Rutherford scattering

$$\tilde{g}(\theta) = \tilde{C} \frac{2\theta}{(a^2 + \theta^2)^2} \quad (40)$$

## 4 Comparison with experimental data

In this section some benchmark comparisons are presented, mainly with experiments deal with electron beams impinging normally on different materials. The simulations were done with Geant4 V8.2

The first benchmark is the comparison with data of Hanson et al. ([12]) which can be seen in Fig.1.

In Fig.2 the lateral spreading of a 2.5 MeV proton beam is shown after mylar foils of different thicknesses. The spreading is measured in a distance 6.3 mm after the foils, the line representing the experimental data have been taken from [13], the squares are the simulation results. The lateral spreading of the beam is directly connected with the angle distribution of the beam after the mylar absorber, so this result is a benchmark comparison for the angle distribution.

Fig. 3 shows the number transmission coefficient  $T$  as function of the foil thickness for 1 MeV electrons in aluminium. The thickness is measured in units of the continuous slowing down range, the data originated from different

measurements have been taken from the review paper of Seltzer and Berger ([14]). The simulation with cut = 0.005 mm (corresponds to 10 keV in energy) reproduces the data quite well.

The next benchmark comparison in Fig. 4 gives the energy deposit distribution of 0.5 MeV electrons in aluminium as a function of depth (depth-dose distribution). The experimental points have been taken from [14], the simulation agrees with the data within errors.

The energy spectra of 1 MeV electrons transmitted through aluminium foils is shown in Fig. 5. The experimental points are from a measurement of Rester and Derrickson ([15]). The simulation again are quite close to the data.

Some backscattering results are shown in Fig. 6, where the backscattering of 41 keV electrons can be seen from different targets. It can be seen that the backscattering is not reproduced without the boundary crossing algorithm and the simulation is close to the data when the value of  $f_r$  becomes small enough.

## 5 Conclusions

A new multiple scattering model has been implemented in Geant4. Despite its simplicity the model is capable to describe the mean properties of the multiple scattering process and reproduce the experimental results well.

## 6 Acknowledgement

I am indebted to M. Maire for enlightening discussions and for his criticism reading the manuscript. I would like to thank the API group of IT and SFT group of PH at CERN for their support.

## References

- [1] Geant4 collaboration *NIM*, **A 506**, p. 250 (2003).
- [2] G. Z. Molière *Z. Naturforsch.*, **3a**, p. 78 (1948).
- [3] J. M. Fernandez-Varea et al. *NIM*, **B73**, p. 447 (1993).
- [4] S. Goudsmit and J. L. Saunderson. *Phys. Rev.*, **57**, p. 24 (1940).
- [5] H. W. Lewis. *Phys. Rev.*, **78**, p. 526 (1950).

- [6] I. Kawrakow and Alex F. Bielajew *NIM*, **B 142**, p. 253 (1998).
- [7] D. Liljequist and M. Ismail. *J.Appl.Phys.*, **62**, p. 342 (1987).
- [8] D. Liljequist et al. *J.Appl.Phys.*, **68**, p. 3061 (1990).
- [9] R.Mayol and F.Salvat *At.Data and Nucl.Data Tables* **65**, p. 55 (1997).
- [10] V.L.Highland *NIM* , **129**, p. 497 (1975).
- [11] G.R. Lynch and O.I. Dahl *NIM*, **B58**, p. 6 (1991).
- [12] A. O. Hanson et al. *Phys. Rev.*, **84**, p. 634 (1951).
- [13] C. Michelet et al. *NIM*, **B181**, p. 157 (2001).
- [14] S. M. Seltzer and M. J. Berger *NIM*, **119**, p. 157 (1974).
- [15] D. H. Rester and J. H. Derrickson *J. Appl. Phys.*, **42**, p. 714 (1971).
- [16] H.J.Hunger and L.Kuchler *Phys.Stat.Sol.(a)*, **56**, K45 (1979).
- [17] G.Shen et al. *Phys. Rev. D* **20 (1979) 1584**.
- [18] D. Attwood et al. *NIM B* **251 (2006) 41**.

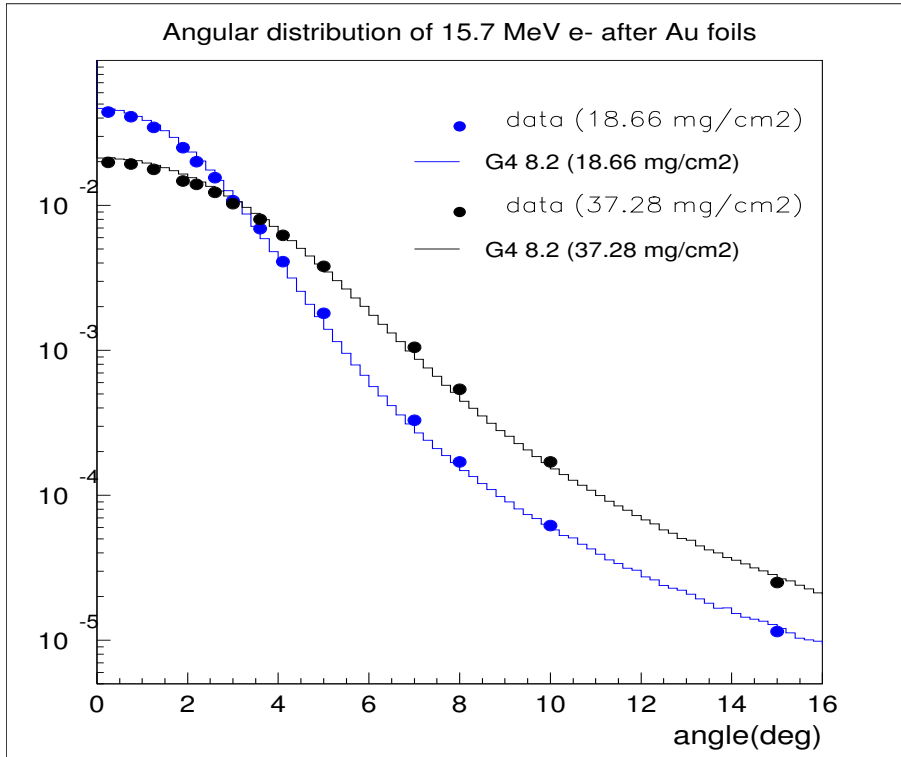


Figure 1: Angular distributions of 15.7 MeV e- transmitted through gold foils; data from [12]

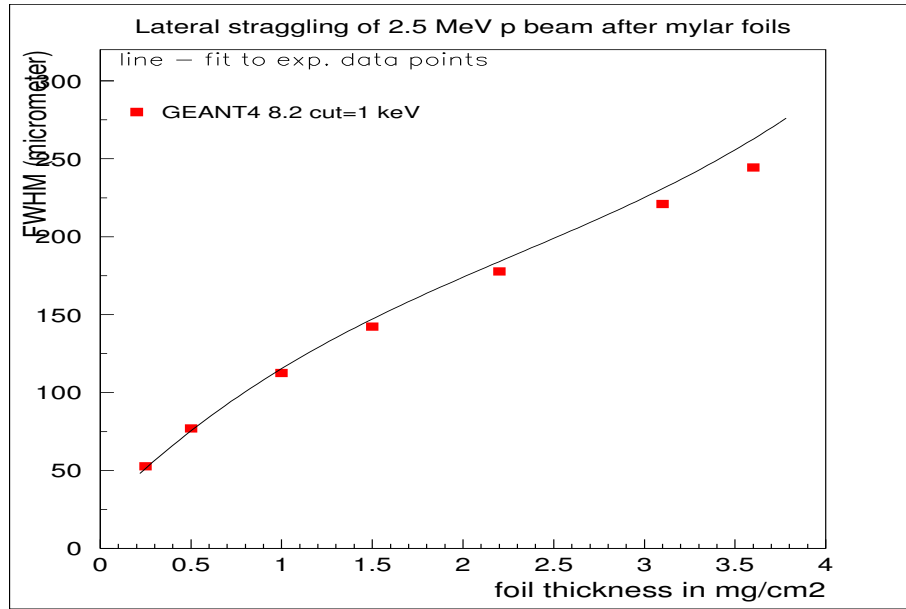


Figure 2: Lateral spreading of 2.5 MeV proton beam after mylar foils; data from [13]

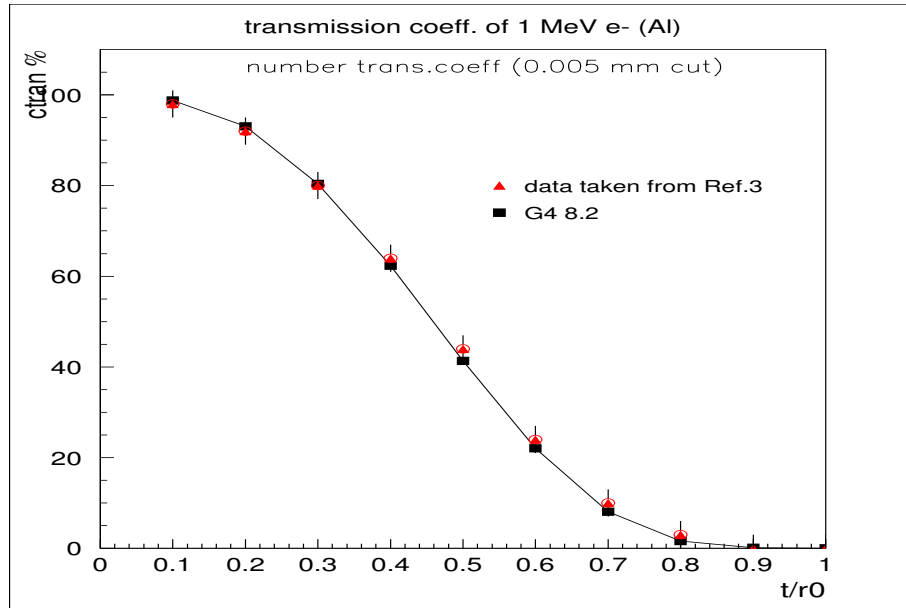


Figure 3: Transmission coeff.  $T$  of 1 MeV  $e^-$  in Al; data from [14].



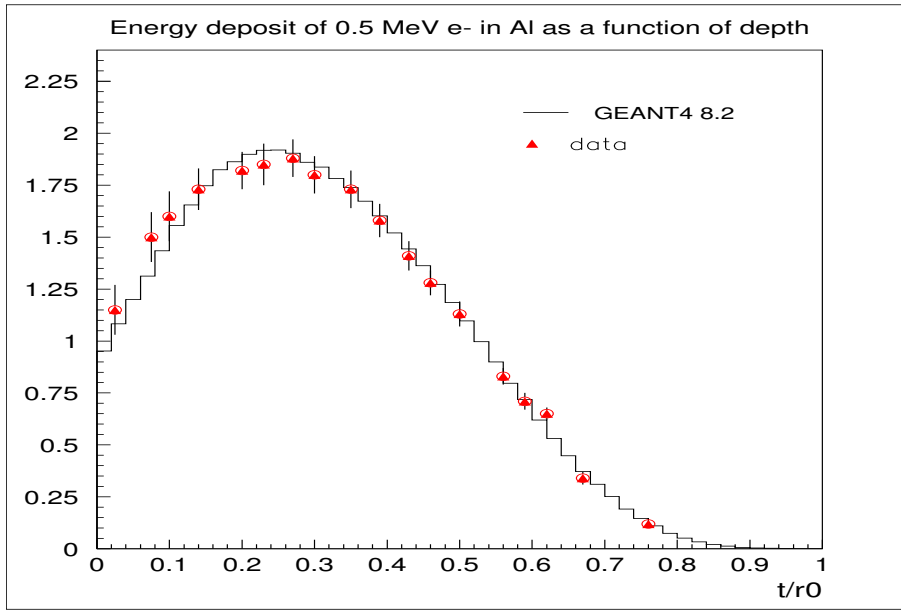


Figure 4: Energy deposit by 0.5 MeV e- in Al, function of depth; data from [14].

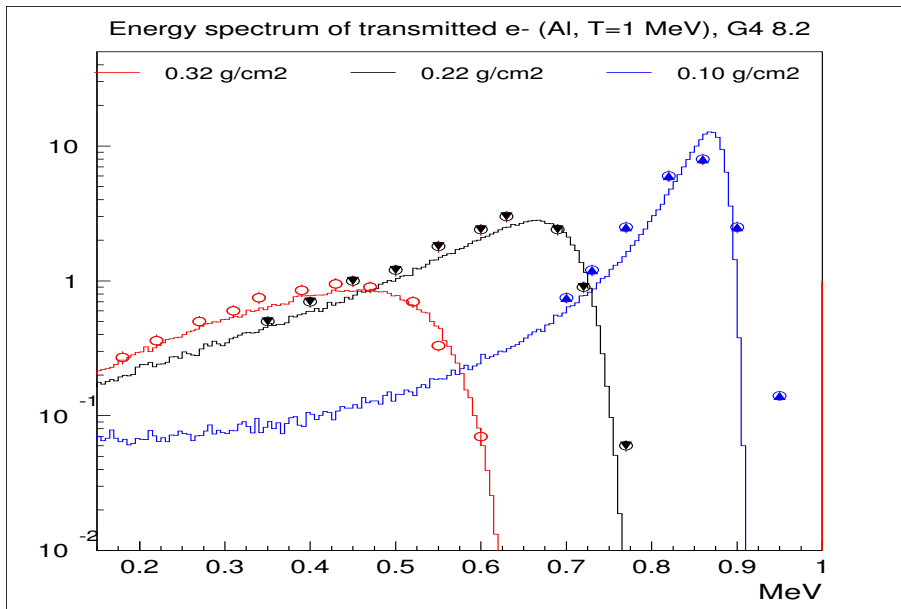


Figure 5: Energy spectrum of 1 MeV e- transmitted through aluminium layers; data from [15].

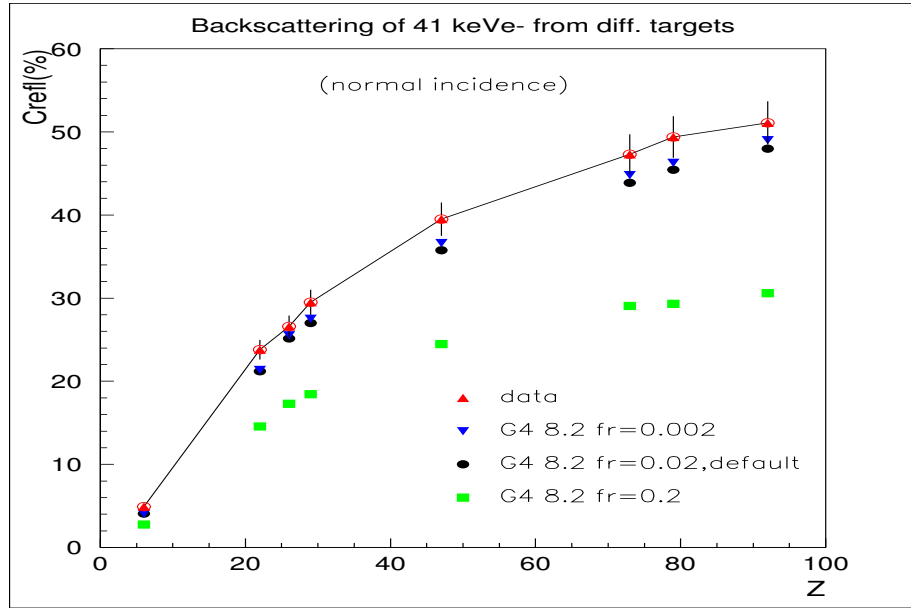


Figure 6: Backscattering coefficients of 41 keV electrons from various targets; data from [16].